Diffraction Loss and Selection of Modes in Maser Resonators with Circular Mirrors

By TINGYE LI

(Manuscript received February 4, 1965)

The losses, phase shifts and field distribution functions for the two lowest-order modes of interferometer-type maser resonators consisting of spherically curved mirrors with circular apertures are computed by solving a pair of integral equations numerically on a digital computer. Solutions are obtained for the symmetric geometry of identically curved mirrors and for the half-symmetric geometry consisting of one plane and one curved mirror, with the radius of curvature of the mirrors as a variable parameter. The confocal or near-confocal configuration is shown to have good mode-selective properties in that the ratio of the loss of the second lowest-order (TEM_{10}) mode to that of the lowest-order (TEM_{00}) mode is the largest of the configurations considered. The numerical results should be of interest to those concerned with the problem of mode selection in optical masers and with the design of single-mode masers with relatively low gain.

I. INTRODUCTION

Interferometer-type resonators used for optical masers usually have a number of modal resonances falling under the gain profile of the active medium. Therefore optical maser oscillators generally can and often do oscillate in many modes, each mode having its own characteristic frequency and field pattern. Such a multimode, multifrequency output is undesirable for applications in communications and metrology. Many mode-selection schemes have been devised and tried, but most of them involve added complications and are beset by problems of stability. A simple solution was obtained by Gordon and White,[1] who built a stable single-frequency gas optical maser using a short, thin discharge tube. The resonator length was made short to reduce the number of longitudinal resonances and the mirror curvature was chosen so that only the lowest-order transverse mode had enough gain for oscillation. (The dif-

fraction losses of the higher-order modes were all greater than the gain of the tube.) Choosing the appropriate mirror curvatures for mode suppression is preferable to the commonly used method of aperturing the mirrors, because the former method does not restrict the amount of active material that can participate in maser action and therefore is capable of producing greater output power.

In order to select a pair of mirrors with the appropriate radii of curvature for single-mode operation, it is important to know accurately the diffraction losses of the modes as functions of the mirror size, spacing and curvature. Much work has been done on resonators with rectangular mirrors: Boyd and Gordon[2] and Boyd and Kogelnik[3] have derived approximate formulas for estimating the losses; Fox and Li[4] have made numerical calculations on a digital computer by solving the appropriate integral equations by the method of successive approximations; Streifer[5] recently made similar calculations using Schmidt expansion theory; Gloge[6] used perturbation techniques for his calculations. Unfortunately, these results are not very practical because the discharge tubes usually have circular cross sections and the diffraction losses for square mirrors and for circular mirrors are not simply related. Recently, Heurtley[7] has made some calculations on the modes and the eigenvalues of resonators with circular mirrors using Schmidt expansion theory. But published data on the diffraction losses suitable for practical design purposes are still lacking. It was with this purpose in mind that we computed the diffraction losses of the two lowest-order modes of the maser resonator with circular mirrors for various mirror curvatures. The results, which complement our earlier work,[4,8,9] should be of interest to those concerned with the problem of mode selection in optical masers.

II. MATHEMATICAL FORMULATION

The geometry of a maser resonator with circular mirrors is shown in Fig. 1. It is convenient to use the cylindrical coordinate system, with its axis coinciding with the axis of the resonator. The mirrors are spherically curved and have radii of curvature equal to R_1 and R_2. The mirror apertures are circular, their radii being a_1 and a_2. The separation between the mirrors along the axis is d.

The integral equations for the modes of the resonator with mirrors of arbitrary curvature and shape are given in Ref. 4. For the present case, they are in the form

$$\gamma^{(1)}\psi^{(1)}(r_1, \varphi_1) = \int_0^{a_2}\int_0^{2\pi} K^{(2)}(r_1, \varphi_1; r_2, \varphi_2)\psi^{(2)}(r_2, \varphi_2) r_2 d\varphi_2 dr_2 \quad (1)$$

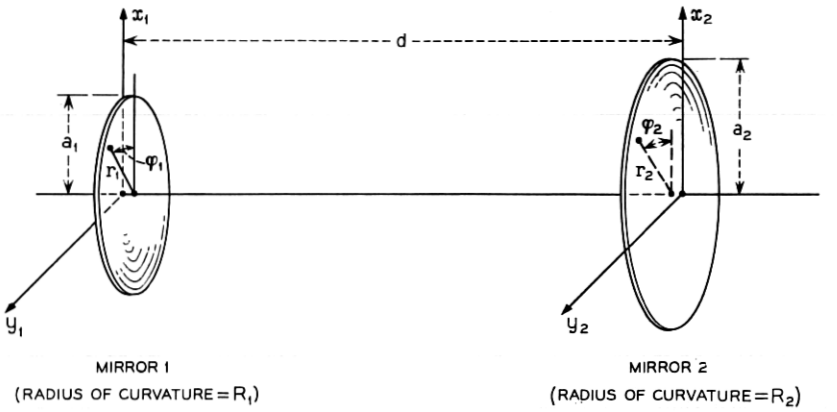

Fig. 1 — Geometry of the maser resonator consisting of spherically curved mirrors with circular mirror apertures.

$$\gamma^{(2)}\psi^{(2)}(r_2, \varphi_2) = \int_0^{a_1}\int_0^{2\pi} K^{(1)}(r_2, \varphi_2; r_1, \varphi_1)\psi^{(1)}(r_1, \varphi_1) r_1 d\varphi_1 dr_1 \quad (2)$$

where $K^{(1)}$ and $K^{(2)}$ are equal and are given by

$$K^{(2)}(r_1, \varphi_1; r_2, \varphi_2) = K^{(1)}(r_2, \varphi_2; r_1, \varphi_1)$$
$$= \frac{j}{\lambda d} \exp\left\{-\frac{jk}{2d}[g_1 r_1^2 + g_2 r_2^2 - 2r_1 r_2 \cos(\varphi_1 - \varphi_2)]\right\}. \quad (3)$$

In the above equations, $\gamma^{(1)}$ and $\gamma^{(2)}$ are the eigenvalues associated with the eigenfunctions $\psi^{(1)}(r_1, \varphi_1)$ and $\psi^{(2)}(r_2, \varphi_2)$, which are distribution functions of the reflected field at each mirror surface; g_1 is equal to $1 - (d/R_1)$ and g_2 is equal to $1 - (d/R_2)$; k is $2\pi/\lambda$ and λ is the wavelength in the medium between the mirrors. Making use of the relation[10]

$$\exp[jn(\pi/2 - \beta)]J_n(xy)$$
$$= \frac{1}{2\pi}\int_0^{2\pi} \exp\{j[xy\cos(\alpha - \beta) - n\alpha]\}\, d\alpha \quad (4)$$

and integrating (1) and (2) with respect to φ_1 and φ_2, respectively, it is seen that

$$\psi^{(1)}(r_1, \varphi_1) = R_n^{(1)}(r_1)e^{-jn\varphi_1}, \qquad (n = \text{integer}) \quad (5)$$

and

$$\psi^{(2)}(r_2, \varphi_2) = R_n^{(2)}(r_2)e^{-jn\varphi_2}, \qquad (n = \text{integer}) \quad (6)$$

satisfy (1) and (2), respectively. Thus the azimuthal variation is sinusoidal in form. The radial functions $R_n^{(1)}(r_1)$ and $R_n^{(2)}(r_2)$ satisfy the reduced integral equations

$$\gamma_n^{(1)} R_n^{(1)}(r_1) \sqrt{r_1} = \int_0^{a_2} K_n(r_1, r_2) R_n^{(2)}(r_2) \sqrt{r_2}\, dr_2 \tag{7}$$

$$\gamma_n^{(2)} R_n^{(2)}(r_2) \sqrt{r_2} = \int_0^{a_1} K_n(r_1, r_2) R_n^{(1)}(r_1) \sqrt{r_1}\, dr_1 \tag{8}$$

where

$$K_n(r_1, r_2) = \frac{j^{n+1}k}{d} J_n\left(k\frac{r_1 r_2}{d}\right) \sqrt{r_1 r_2} \exp\left\{-\frac{jk}{2d}(g_1 r_1^2 + g_2 r_2^2)\right\} \tag{9}$$

and J_n is a Bessel function of the first kind and nth order. It is unnecessary to show that the modes are orthogonal over their respective mirror surfaces, since this has been demonstrated for the general case of arbitrary mirrors.[4]

III. COMPUTED RESULTS AND DISCUSSION

An IBM 7094 computer was programmed to solve (7) and (8) for the two lowest-order modes (TEM_{00} and TEM_{10}) and their eigenvalues using the method of successive approximations.[4,8] Solutions were obtained for the symmetric and half-symmetric geometries; the symmetric geometry consists of identical mirrors ($a_1 = a_2 = a$, $g_1 = g_2 = g$) and the half-symmetric geometry consists of one plane and one curved mirror ($a_1 = a_2 = a$, $g_1 = 1.0$). In all cases, fifty or more intervals were used for the numerical integration of (7) and (8). When the losses were low and the convergence was slow, as many as one hundred intervals were used.

Figs. 2 and 3 show the relative field distributions of the lowest-order (TEM_{00}) and the next lowest-order (TEM_{10}) modes for the symmetric case. Except for geometries close to plane-parallel or concentric ($g \approx \pm 1$), the relative amplitude distributions can be closely approximated by Gaussian-Laguerre functions, with the spot sizes of the TEM_{00} mode equal to $(\lambda d/\pi)^{\frac{1}{2}}(1 - g^2)^{-\frac{1}{4}}$, as given by Boyd and Gordon.[2] Also, for geometries other than plane-parallel or concentric, the equiphase surfaces almost coincide with the mirror surfaces. The agreement between the computed field distributions and those of the generalized confocal theory[2,3] becomes closer with larger Fresnel numbers ($N > 1$).

The power losses per transit of the two lowest-order modes are given in Figs. 4 and 5 for various values of g lying in the low-loss region

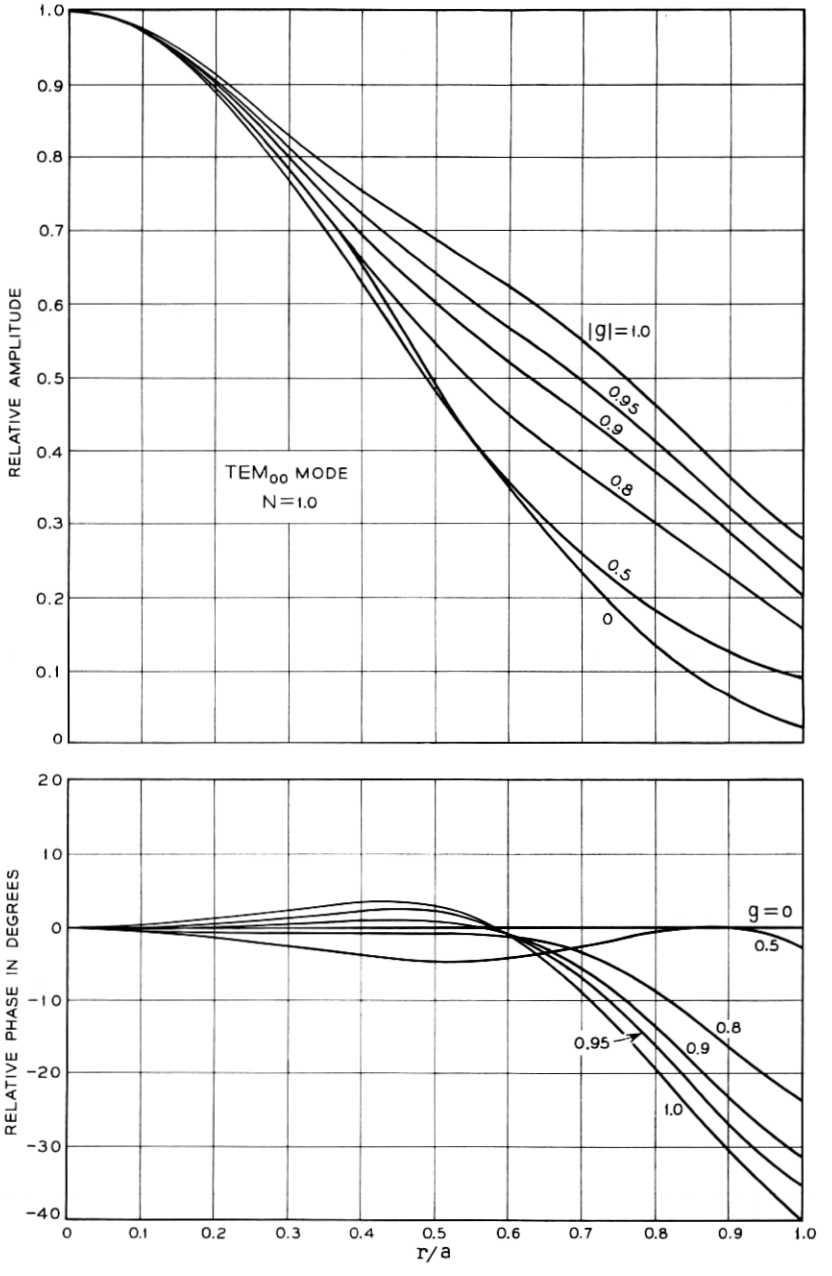

Fig. 2 — Relative field distributions of the fundamental (TEM_{00}) mode for the symmetric geometry ($N = a^2/\lambda d = 1.0$).

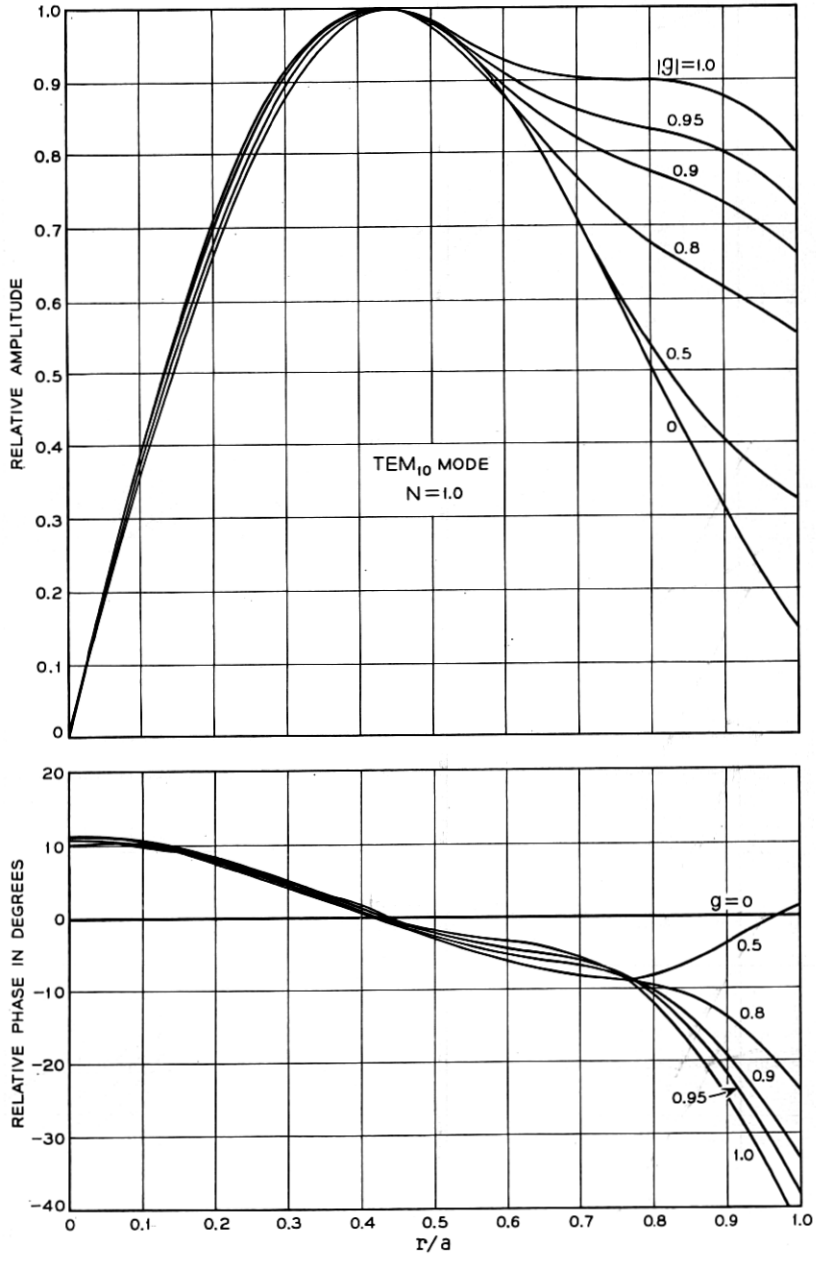

Fig. 3—Relative field distributions of the TEM_{10} mode for the symmetric geometry ($N = a^2/\lambda d = 1.0$).

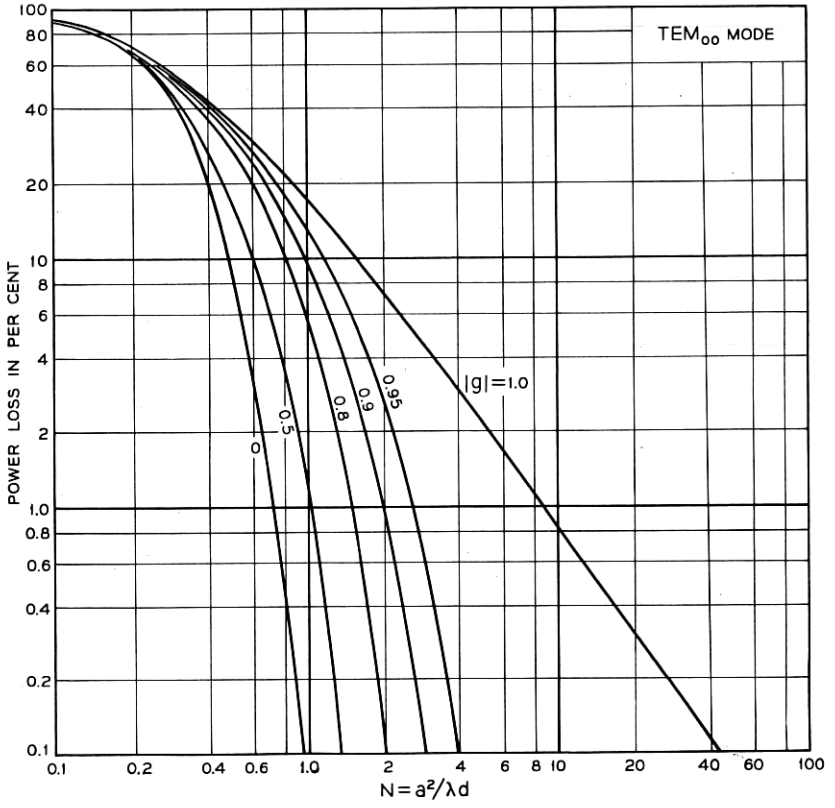

Fig. 4 — Power loss per transit of the fundamental (TEM_{00}) mode for the symmetric geometry.

($0 \leqq |g| \leqq 1$).[3,4] The curves for $|g| = 1$ (plane-parallel or concentric) and $g = 0$ (confocal) are the same as those given previously by Fox and Li.[8] Curves for other values of g lie between these two. The computed loss values for the confocal configuration are in perfect agreement with those of Slepian,[11] who has obtained various analytical expressions to approximate the losses. For our interest, the most useful form of the expression for the loss of the TEM_{nm} mode obtained by Slepian is

$$\text{loss} = \frac{2\pi(8\pi N)^{2m+n+1}e^{-4\pi N}}{\Gamma(m+1)\Gamma(m+n+1)} \cdot \left[1 + \frac{\text{constant}}{2\pi N} + \text{higher-order terms in } \frac{1}{2\pi N}\right] \tag{10}$$

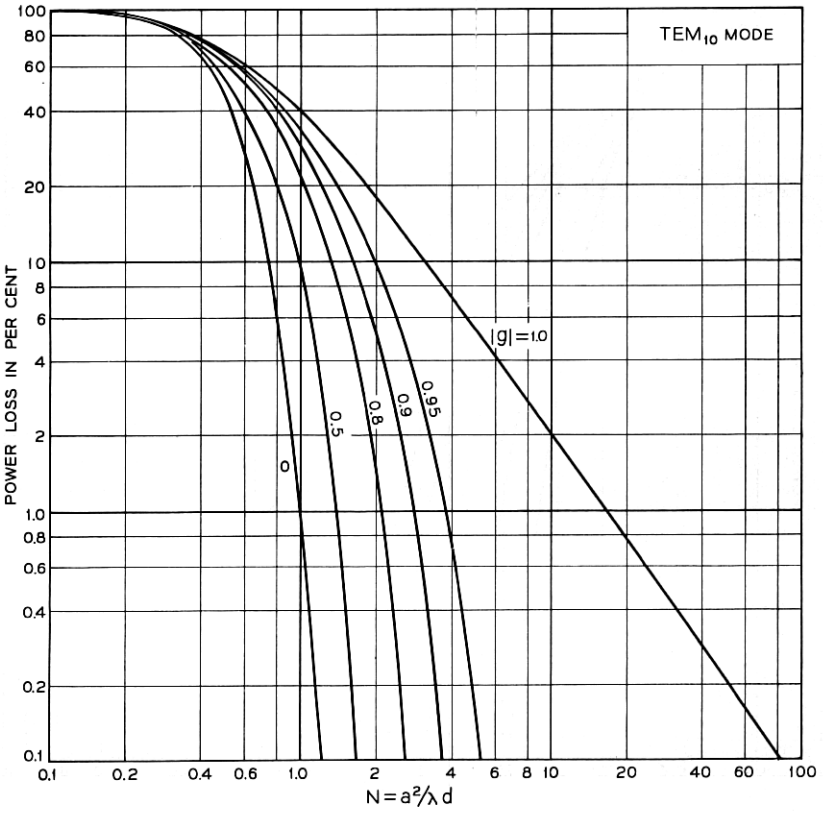

Fig. 5 — Power loss per transit of the TEM_{10} mode for the symmetry geometry.

where n and m are the azimuthal and the radial mode numbers respectively, and $\Gamma(x)$ is the gamma function. The computed curves for the plane-parallel or the concentric configuration are in excellent agreement with those of Vainshtein,[12] who has obtained an approximate formula for the loss of the TEM_{nm} mode. It is of the form

$$\text{loss} = 8\nu_{nm}^2 \frac{\beta(M + \beta)}{[(M + \beta)^2 + \beta^2]^2} \tag{11}$$

where ν_{nm} in the mth zero of the Bessel function $J_n(x)$, $\beta = 0.824$ and $M = (8\pi N)^{\frac{1}{2}}$. Both formulas (10) and (11) fail for small Fresnel numbers where losses are appreciable.

It is seen from Figs. 4 and 5 that the diffraction losses are very sensitive to changes in mirror curvature; also, provided $|g|$ is not very close

to unity, the losses decrease very rapidly as N increases. By choosing g and N suitably, it is possible to have a strongly oscillating fundamental mode in an optical maser with all higher-order modes suppressed. For example, if a maser tube has a gain of five per cent and the Fresnel number of the resonator is two, higher-order modes will not oscillate with $g = 0.90$. (Loss of TEM_{00} mode $\approx$1 per cent and loss of TEM_{10} mode $\approx$5.2 per cent).

While the loss of each mode is given by the magnitude of its eigenvalue, its resonant frequency is determined by the phase of its eigenvalue, which is equal to the phase shift (relative to the geometrical phase shift) per transit for the mode. The phase shifts for the two lowest-order modes are plotted in Figs. 6 and 7. The curves shown are for positive g only;

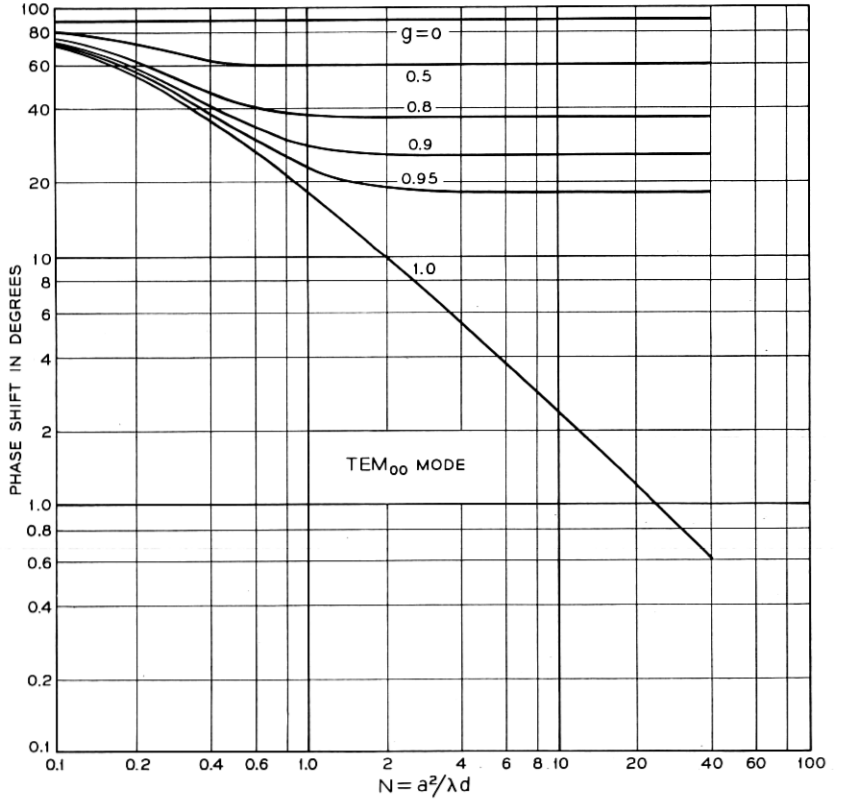

Fig. 6 — Phase shift per transit (leading relative to the geometrical phase shift) of the fundamental (TEM_{00}) mode for the symmetric geometry.

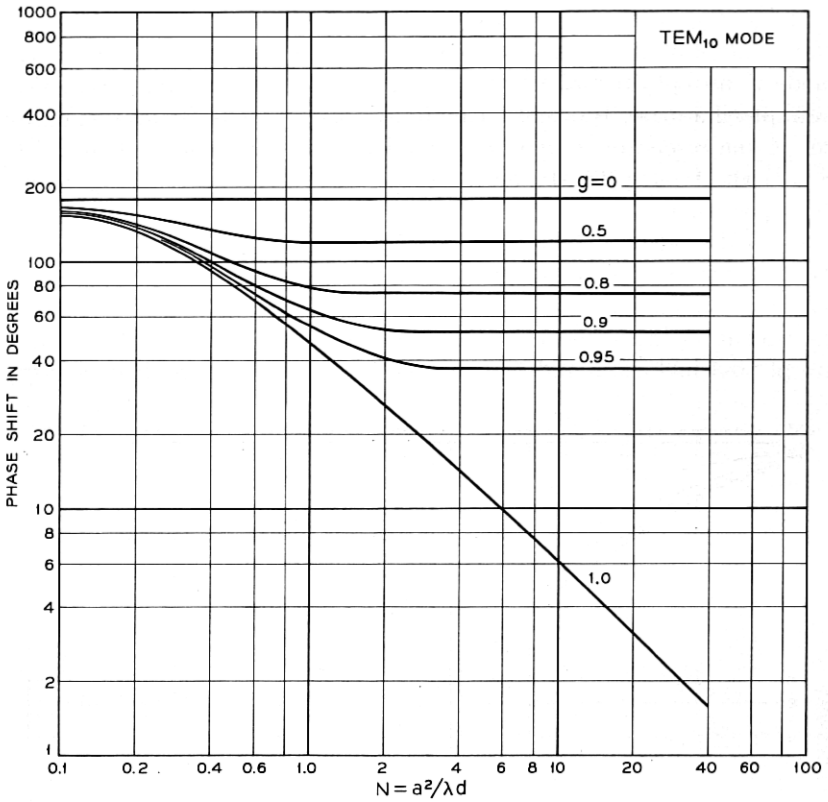

Fig. 7 — Phase shift per transit (leading relative to the geometrical phase shift) of the TEM_{10} mode for the symmetric geometry.

the phase shift for negative g is equal[4] to 180 degrees minus that for positive g. The horizontal portions of the curves can be calculated from the theory of Boyd and Kogelnik[3] as

$$\begin{aligned} \text{phase shift} &= (2m + n + 1) \arccos \sqrt{g_1 g_2} \\ &= (2m + n + 1) \arccos g, \quad \text{for} \quad g_1 = g_2 . \end{aligned} \tag{12}$$

The problem of mode discrimination in an optical maser can be approached in two different ways which depend on the available gain of the active medium. If the gain is large, the relative magnitudes of the eigenvalues of the different modes are of importance.[13,14,15] On the other hand, if the gain is small, such as in 6328Å He-Ne masers, the relative losses are important.[9] The ratio of the loss of the TEM_{10} mode to the loss

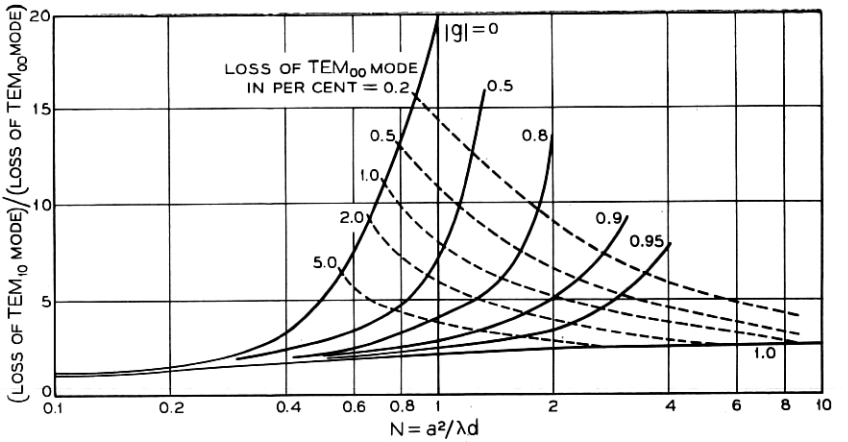

Fig. 8 — Ratio of the losses per transit of the two lowest-order modes for the symmetric geometry. The dotted curves are contours of constant loss for the TEM_{00} mode.

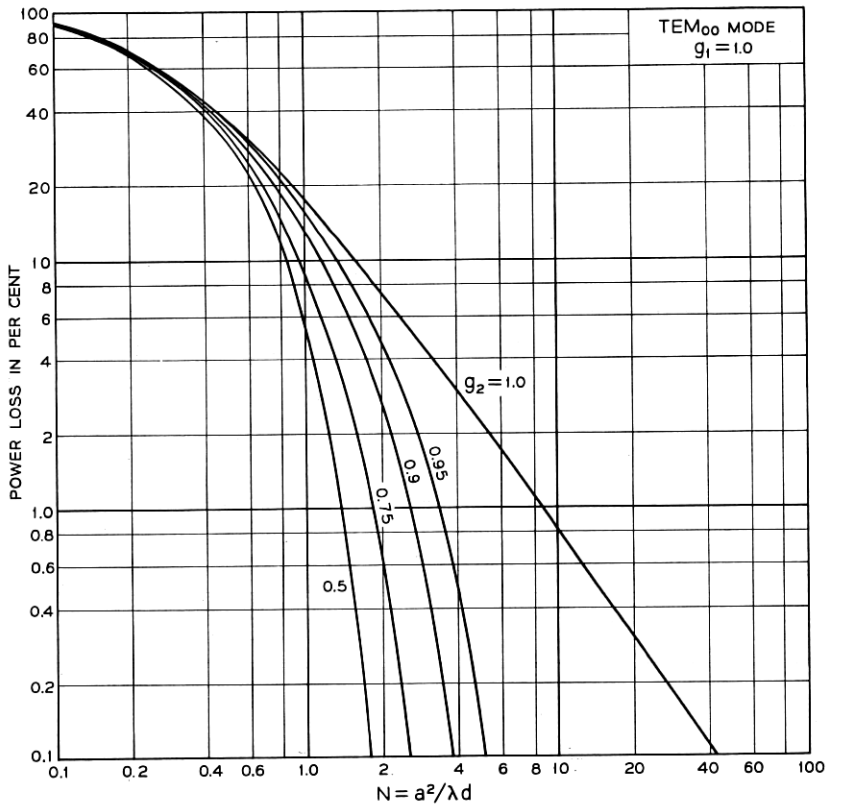

Fig. 9 — *Average* power loss per transit of the fundamental (TEM_{00}) mode for the half-symmetric geometry.

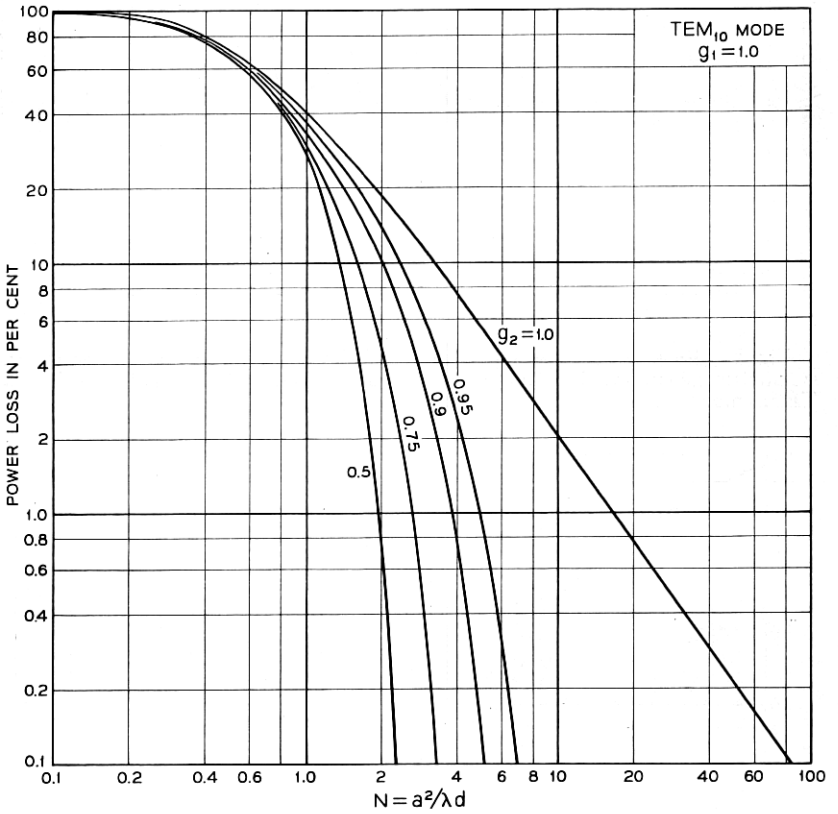

Fig. 10 — *Average* power loss per transit of the TEM_{10} mode for the half-symmetric geometry.

of the TEM_{00} mode, which is a measure of mode selectivity for the low-gain case, is plotted in Fig. 8 as functions of the Fresnel number. The dotted curves are contours of constant loss for the TEM_{00} mode. It is clear from this plot that the confocal or near-confocal geometry possesses good mode-selective properties, and that the plane-parallel or the concentric geometry is rather poor. However, if an aperture is placed in the midplane of a concentric resonator, its mode-selective properties have been shown to improve and to approach the confocal resonator.[9]

One of the commonly used resonator configurations is the half-symmetric geometry consisting of one plane and one curved mirror. If the spot size of the mode pattern at the plane mirror is very much smaller than the effective mirror aperture, such as in the case of the half-con-

centric or near half-concentric configuration, the half-symmetric resonator can be regarded as equivalent to a symmetric resonator of twice the length. However, if the mirror configuration is such that it lies between the half-confocal and the plane-parallel ($g_1 = 1.0$ and $0.5 \leqq g_2 \leqq 1.0$) and the effective mirror apertures are the same, the equivalence of half-symmetric and symmetric resonators is not valid and the modes and their eigenvalues must be recomputed. Computations were carried out for $g_1 = 1.0$ and $g_2 = 0.5$, 0.75, 0.9 and 0.95 corresponding to $g = 0$, 0.5, 0.8 and 0.9 of the symmetric case. Since the mode pattern at the plane mirror is now different from that at the curved mirror, the losses and the phase shifts incurred at the mirrors are also different. As before,[4] we define the *average* loss per transit as $1 - |\gamma^{(1)}\gamma^{(2)}|$ and the *average* phase

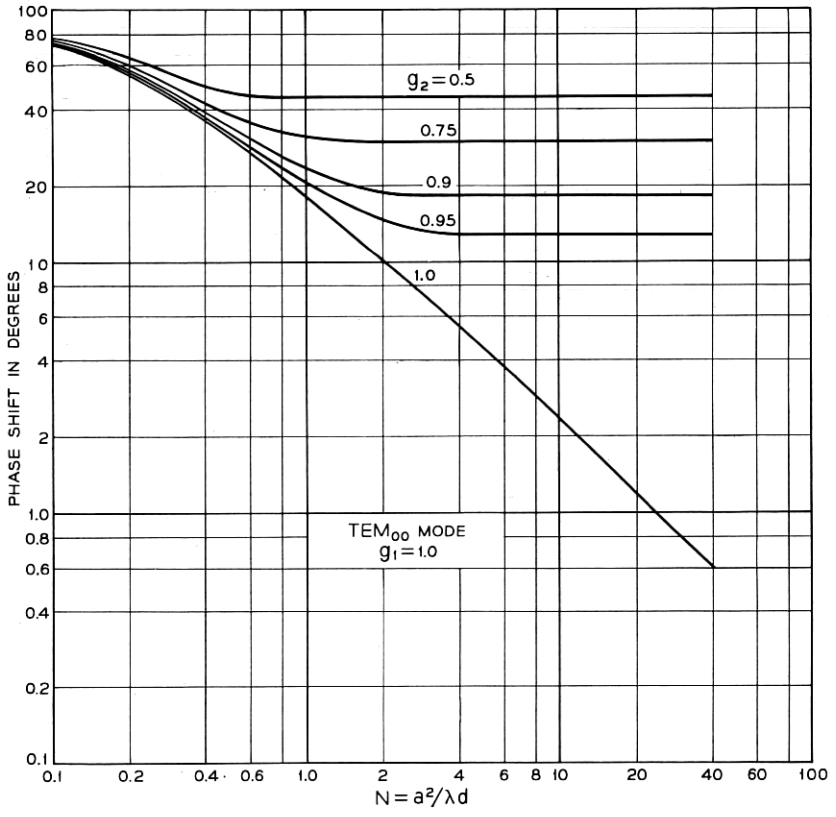

Fig. 11 — *Average* phase shift per transit (leading relative to the geometrical phase shift) of the fundamental (TEM_{00}) mode for the half-symmetric geometry.

shift per transit as (phase of $\gamma^{(1)}$ + phase of $\gamma^{(2)}$)/2. The computed average losses and average phase shifts per transit for the two lowest-order modes are given in Figs. 9 to 12, which are to be compared with those of the symmetric geometry shown in Figs. 3 to 6. The ratio of the loss of the TEM_{10} mode to the loss of the TEM_{00} mode for the half-symmetric resonator is plotted in Fig. 13. Comparing Figs. 8 and 13, it is seen that the mode-selective properties of the half-symmetric resonator are very similar to those of the corresponding symmetric resonator.

Although the computed results are for equal mirror apertures ($a_1 = a_2$), they are also applicable to certain "equivalent" geometries with unequal mirror apertures. The equivalence relations are discussed and given in a recent paper by Gordon and Kogelnik.[16]

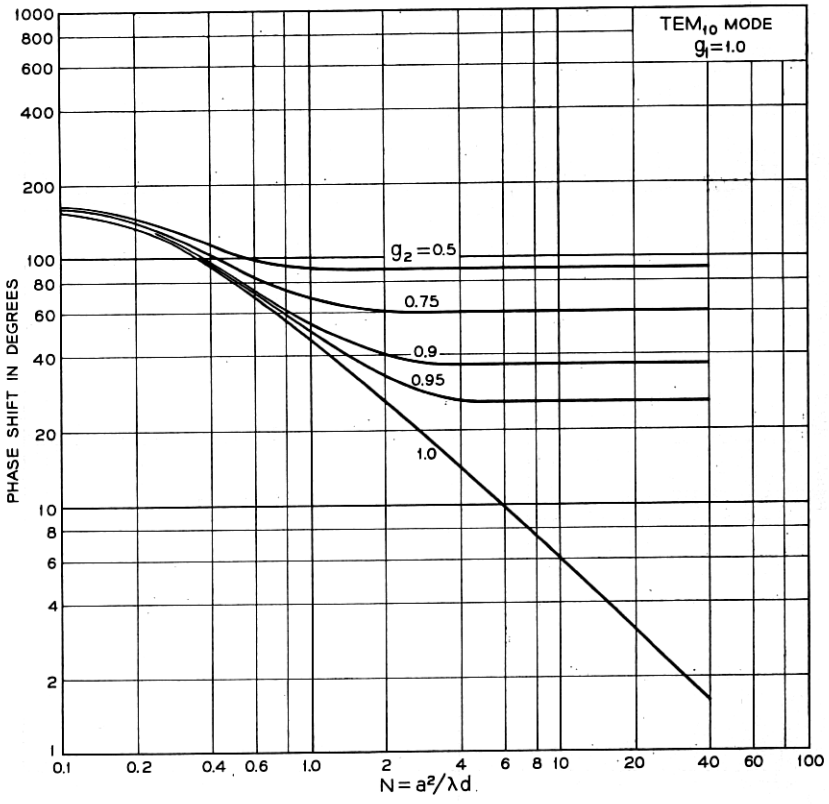

Fig. 12 — *Average* phase shift per transit (leading relative to the geometrical phase shift) of the TEM_{10} mode for the half-symmetric geometry.

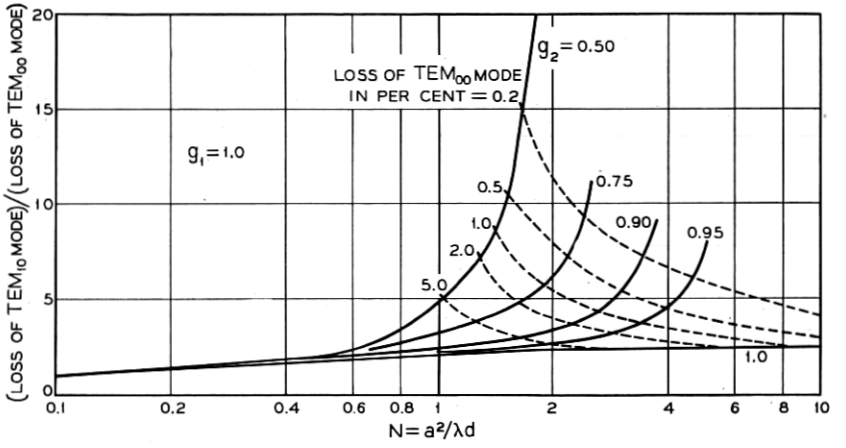

FIG. 13 — Ratio of the *average* losses per transit of the two lowest-order modes for the half-symmetric geometry. The dotted curves are contours of constant *average* loss for the TEM_{00} mode.

IV. CONCLUSIONS

The diffraction losses of the modes of interferometer-type maser resonators can be utilized for mode discrimination. Results of the computation show that the confocal or near-confocal resonator has good mode-selective properties; but its mode volume is small compared with those of the plane-parallel or concentric resonator of the same Fresnel number.[2,17,18] Since it is desirable to utilize as much of the active material as possible in order to obtain the maximum output power from a maser, a geometry that is as close to plane-parallel as is consistent with the requirements of mode discrimination and mechanical stability is to be preferred. In practice, the perturbing effects of the maser tube wall, the mirror irregularities, the nonlinearity of the active medium, etc. will modify the idealized modes and their losses and therefore should be taken into consideration.

V. ACKNOWLEDGMENT

The computational assistance of Mrs. C. L. Beattie is gratefully acknowledged.

REFERENCES

1. Gordon, E. I., and White, A. D., Single-Frequency Gas Lasers at 6328A, Proc. IEEE, *52*, Feb., 1964, p. 206.

2. Boyd, G. D., and Gordon, J. P., Confocal Multimode Resonator for Millimeter through Optical Wavelength Masers, B.S.T.J., *40*, March, 1961, p. 489.
3. Boyd, G. D., and Kogelnik, H., Generalized Confocal Resonator Theory, B.S.T.J., *41*, July, 1962, p. 1347.
4. Fox, A. G., and Li, Tingye, Modes in a Maser Interferometer with Curved and Tilted Mirrors, Proc. IEEE, *51*, Jan., 1963, p. 80.
5. Streifer, W., Modes in Spherical Resonators with Rectangular Mirrors, J. Opt. Soc. Am., *54*, Nov., 1964, p. 1399.
6. Gloge, D., Calculations of Fabry-Perot Laser Resonators by Scattering Matrices, Arch. Elekt. Ubertragung, *18*, March, 1964, p. 197.
7. Heurtley, J. C., Optical Resonators with Circular Mirrors, J. Opt. Soc. Am., *54*, Nov., 1964, p. 1400.
8. Fox, A. G., and Li, Tingye, Resonant Modes in a Maser Interferometer, B.S.T.J., *40*, March, 1961, p. 453.
9. Li, Tingye, Mode Selection in an Aperture-Limited Concentric Maser Interferomteter, B.S.T.J., *42*, Nov., 1963, p. 2609.
10. Stratton, J. A., *Electromagnetic Theory*, McGraw-Hill, New York, 1941, p. 372.
11. Slepian, D., Prolate Spheroidal Wave Functions, Fourier Analysis and Uncertainty — IV: Extensions to Many Dimensions; Generalized Prolate Spheroidal Functions, B.S.T.J., *43*, Nov. 1964, p. 3009.
12. Vainshtein, L. A., Open Resonators for Lasers, JETP (USSR), *44*, March, 1963, p. 1050; Sov. Phys. JETP, *17*, Sept. 1963, p. 709.
13. LaTourette, J. T., Jacobs, S. F., and Rabinowitz, P., Improved Laser Angular Brightness Through Diffraction Coupling, Appl. Opt., *3*, August, 1964, p. 981.
14. Barone, S. R., and Newstein, M. C., Fabry-Perot Resonances at Small Fresnel Numbers, Appl. Opt., *3*, Oct., 1964, p. 1194.
15. Siegman, A. E., Unstable Optical Resonators for Laser Applications, Proc. IEEE, *53*, March, 1965, p. 277.
16. Gordon, J. P., and Kogelnik, H., Equivalence Relations among Spherical Mirror Optical Resonators, B.S.T.J., *43*, Nov., 1964, p. 2873.
17. Sinclair, D. C., Choice of Mirror Curvatures for Gas Laser Cavities, Appl. Opt., *3*, Sept., 1964, p. 1067.
18. Clark, P. O., A Self-Consistent Field Analysis of Spherical-Mirror Fabry-Perot Resonators, Proc. IEEE, *53*, Jan., 1965, p. 36.